Journal of Neonatal Surgery
ISSN(Online): 2226-0439
Vol. 14, Issue 31s (2025)
https://www.jneonatalsurg.com

OPEN ACCESS

Fabrication Of Cobalt Oxide Nanoparticles Using Barringtonia Acutangula For Evaluation Of Antibacterial, Antioxidant And Protein Denaturation Activities

Jeyapaul Ashli[1a], Subramanian Priya Velammal*[b], Thomas Peter Amaladhas[c]

[a]Research Scholar, Reg.No.19232232032009, Department of Chemistry, V. O. Chidambaram College, Tuticorin, Tamil Nadu 628 008, India, Affiliated to Manonmaniam Sundaranar University, Abishekapatti, Tirunelveli-627012, Tamilnadu, India.

[b]Associate Professor, Department of Chemistry, V. O. Chidambaram College, Tuticorin, Tamil Nadu 628 008, India, Affiliated to Manonmaniam Sundaranar University, Abishekapatti, Tirunelveli-627012, Tamilnadu, India.

[c]Principal, Malankara Catholic College, Mariagiri, Kaliyakkavilai, 629153, Kanyakumari, Tamil Nadu, India.

[*]**Corresponding author:**

Subramanian Priya Velammal

Email ID: subraja1950@gmail.com

Cite this paper as: Jeyapaul Ashli, Subramanian Priya Velammal, Thomas Peter Amaladhas, (2025) Fabrication Of Cobalt Oxide Nanoparticles Using Barringtonia Acutangula For Evaluation Of Antibacterial, Antioxidant And Protein Denaturation Activities. *Journal of Neonatal Surgery*, 14 (31s), 495-506.

ABSTRACT

Nanocobalt oxide particles were fabricated through an uncomplicated and sustainable process using dried fruit extract from *Barringtonia acutangula*. The successful formation of nanoparticles was evidenced by a characteristic absorption band observed between 300 to 750 nm. The presence of natural phytochemicals such as polyphenols and triterpenoids, which served as stabilizing agents by binding to the nanoparticle surface and supporting the formation of a stable Cobalt oxide lattice was confirmed using FTIR analysis. XRD analysis revealed the crystalline structure consistent with cobalt oxide. SEM images showed that the nanoparticles exhibited rough and irregular surface morphologies. EDX analysis confirmed uncontaminated state of the sample. The size was calculated to be 43 nm using TEM analysis. Additionally, the Cobalt oxide nanoparticles produced through the biological method worked against four different bacterial strains. They showed 91.27 % antioxidant activity and 59.6 % inhibition activity.

Keywords: *Barringtonia acutangla, Nanocobalt oxide particles, Antibacterial activity, Antioxidant activity, Protein denaturation studies.*

1. INTRODUCTION

Nanotechnology has become a revolutionary field with wide-ranging uses in medicine, environmental science, electronics, and catalysis. Among the different nanomaterials, cobalt oxide nanoparticles have attracted considerable interest their remarkable physicochemical features, like immense surface area, magnetic properties, redox activity etc., These features make cobalt oxide nanoparticles highly appropriate for catalytic processes, sensor development, energy preservation and medical fields [1].

Conventional synthesis methods for cobalt oxide nanoparticles often rely on harmful chemicals, consume substantial energy, and produce environmentally damaging waste. In contrast, green synthesis approaches employ biological agents such as plant extracts, microorganisms, and biomolecules, providing a more sustainable and environmentally friendly alternative. This approach supports green chemistry principles by focusing on lower toxicity, renewable materials, and energy conservation [2]. Using plants to synthesize cobalt oxide nanoparticles is especially promising due to the rich presence of phytochemicals like polyphenols, alkaloids, flavonoids, and terpenoids that naturally facilitate reduction and stabilization processes. The bioactive substances not only help convert cobalt salts into nanoparticles but also affect their shape and stability [3]. Furthermore, nanoparticles produced through green methods often demonstrate improved biocompatibility and functionality, enhancing their suitability for biomedical and environmental uses [4].

In application, green-synthesized cobalt oxide nanoparticles have proven effective in various areas. They act as photocatalysts for breaking down organic pollutants, function as electrode components in Li-batteries and super

electrochemical capacitors and function as antimicrobial agents by damaging microbial cell membranes [5]. Their eco-friendly production process adds to their attractiveness for sustainable technologies.

Barringtonia acutangula, known as freshwater mangrove or Indian oak, is a multipurpose plant valued for its traditional, medicinal, and ecological roles. Used in Ayurvedic and folk medicine, its bark, leaves, and seeds have antibacterial, anti-inflammatory, antidiabetic, and antiparasitic properties, treating infections, wounds, digestive issues, and pain. This study focuses on exploring green synthesis techniques for cobalt oxide nanoparticles using various biological sources and assessing their diverse applications, with a special emphasis on biomedical uses.

2. MATERIALS AND METHODS

2.1. Chemicals

Cobalt (II) Nitrate Hexahydrate of Analytical Reagent (AR) grade with 99% purity (Extrapure AR, ACS standard) was procured from SRL Pvt. Ltd., Chennai. The compound was utilized directly without further refinement. Unless mentioned otherwise, all experimental procedures were carried out using double distilled water.

2.2. Plant materials

The dried fruits of *Barringtonia acutangula*, locally referred to as Brown Samudra was procured from a Siddha medicinal store in Thoothukudi district. The collected botanical specimen was taxonomically identified as *Barringtonia acutangula*. The fruit material was subsequently pulverized using a mechanical grinder and passed through a sieve to obtain powder. The resultant dried fruit powder was stored under appropriate conditions and utilized for the preparation of the plant extract.

Fig. 1 (a) Cobalt(II)nitrate hexahydrate (b) Dried fruits and (c) Powder of *Barringtonia acutangular*

2.3. Preparation of Cobalt oxide nanoparticles using *Barringtonia acutangla*

Precisely 10 grams of sun-dried *Barringtonia acutangula* fruit powder was subjected to aqueous extraction by maintaining the temperature less than 100°C for 30 min with continuous stirring. Whatman No. 41 filter paper was employed to filter resultant extract, then labelled appropriately, maintained at a temperature below 5^0C to use subsequently in nanoparticle synthesis.

About 100 millilitre of the prepared plant extract was gradually added to 100 millilitre of a 1/10 M aqueous solution of cobalt (II) nitrate hexahydrate with uninterrupted mixing using magnetic stirrer at 80 °C throughout 1 hr. The formation of a precipitate indicated the initiation of nanoparticle synthesis which was then isolated by centrifugation and placed in a muffle furnace throughout 2 hr for thermal treatment (calcination) at 600 °C. The resulting black cobalt oxide nanoparticles were collected, dried, and stored under appropriate conditions for physicochemical characterization and potential application studies.

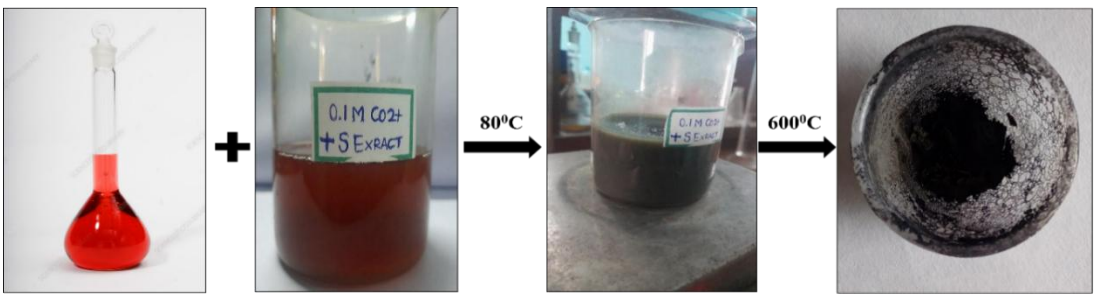

Fig 2. *Synthesis of Cobalt oxide nanoparticles*

2.4. Antibacterial activity

A loopful of microbial culture was inoculated into 10 mL of sterilized substrate Agar. At about 37 °C, the bacterial variants were incubated and fungal strains were maintained 30 °C. *Aspergillus niger* was cultured on an acidified PDA slant. For antimicrobial testing, 25 millilitre of sterile Agar (Mueller-Hinton) was transferred into petri dishes and cooled to solidification, followed by uniform inoculation with the test organisms.

Disc diffusion method which evaluates the antibacterial activity, used discs of aseptic filter papers that were loaded with 15 µL of plant or animal extracts and standard drugs. It was then placed on the inoculated agar, ensuring no overlap between inhibition zones. The inoculated petri discs were cultured at 37 °C for a day and at 30 °C for 2 days for bacteria and fungi respectively [6]. Post-incubation, measurements of the inhibition zones were taken in millimetres.

$$\text{Active Index (AI)} = \frac{Zone\ of\ inhibition\ of\ sample}{Zone\ of\ inhibition\ of\ standard} * 100$$

2.5. Anti-oxidant activity

The overall antioxidant potential was evaluated through the Phospho-Molybdenum assay (Prieto et al.). A standard calibration plot was constructed using known concentrations of ascorbic acid (ranging from 31.25 to 1000 µg/mL dissolved in methanol). During the test procedure, 1.0 gram of cobalt oxide nanoparticles was combined with 1.0 milliliter of reagent mixture (comprising 4 mM ammonium heptamolybdate, 28 mM trisodium phosphate and 6/10 M H_2SO_4) and kept at 95°C for 90 min, The absorbance readings were taken at a wavelength of 695 nm when samples were allowed to cool to room temperature. Milligrams of ascorbic acid equivalent (AAE) for every gram of nanoparticle sample was the measure that was used to quantify percentage antioxidant efficacy with the following equation,

$$\text{Antioxidant activity} = \frac{As}{Ac} \text{ x } 100$$

were A_c is the absorbance of the control while A_s is the absorbance of the sample.

2.6. Protein denaturation inhibition activity

Test solution (1 mL) was combined with cobalt oxide nanoparticles (0–1000 µg/mL) along with 1 mL each of BSA (1%) and buffer of phosphate. It was maintained at 37 ± 1 °Celsius for 30 minutes, after which heat-induced denaturation was carried out at 57 °C, placed in a temperature-controlled water bath for another 30 min. Upon cooling, a spectrophotometer was employed to quantify the turbidity at 660 nm. The percentage inhibition of protein denaturation of the test sample (A_t) was determined relative to the control (A_c) sample lacking nanoparticles and the outcome is presented.

$$\%\ \text{Inhibition} = \frac{Ac - At}{Ac} \text{x } 100$$

2.7. Characterization techniques

A comprehensive characterization of the synthesized materials was undertaken using a suite of analytical techniques. The morphology of the samples was explored through scanning electron microscopy (SEM), conducted with a Carl Zeiss EVO 18 at 15 kV under standard imaging conditions. Elemental composition was determined via energy-dispersive X-ray spectroscopy (EDX), employing a Quantax 200 system integrated with a Bruker X-Flash detector. To investigate internal structure and particle size, high-resolution images were obtained using transmission electron microscopy (TEM) on a JEOL JEM-2100 Plus. Crystallographic analysis and phase identification were achieved through X-ray diffraction (XRD) using a Bruker ECO D8 ADVANCE diffractometer, scanning across a 2θ range of 10° to 90°, and the average crystallite size was estimated using the Debye-Scherrer equation. Functional groups present in the materials were identified by collecting Fourier-transform infrared (FT-IR) spectra with a Nicolet iS5 spectrometer. Additionally, the optical properties were evaluated using a JASCO V-650 UV-Visible spectrophotometer, which was operated under computer control.

3. RESULTS AND DISCUSSION

3.1. Ultraviolet-Visible analysis of Cobalt oxide nanoparticles

As depicted in Figure 3(a), the ultraviolet visible spectrum of *Barringtonia acutangula* extract displays two distinct absorption peaks as result of electronic transitions: a broad one near 253.5 nm is attributed to π–π* and another peak at 358 nm could be assigned to n–π* respectively, arising from various phytochemicals present in the extract. The presence of both peaks suggests a high concentration of triterpenoids, which are known to strongly absorb UV light. This observation aligns with existing studies indicating that plant extracts rich in triterpenoids typically exhibit dual peaks at 230–280 nm and 300–550 nm. Figure 3(b) demonstrates the optical property of cobalt oxide nanoparticles, with a broad absorption band in the 200–800 nm range. This absorption is attributed to electronic transitions between the valence and conduction bands in the nanoparticles. The optical absorption observed within the wavelength ranges of 300–700 nm corresponds to electronic transitions involving oxygen and cobalt ions. Specifically, these can be attributed to transitions from the O^{2-} 2p orbitals to

the Co^{2+} t_2 orbitals and to the Co^{3+} e_g orbitals. These represent the material's bandgap energy transitions. The valence band is predominantly composed of oxygen 2p states, while the conduction band is primarily formed by Co^{2+} 3d orbitals, which contribute most of the charge carriers [8-10]. Overall, the spectral features observed between 300–750 nm confirm the presence of both Co^{2+} and Co^{3+} in nanocobalt oxide particles.

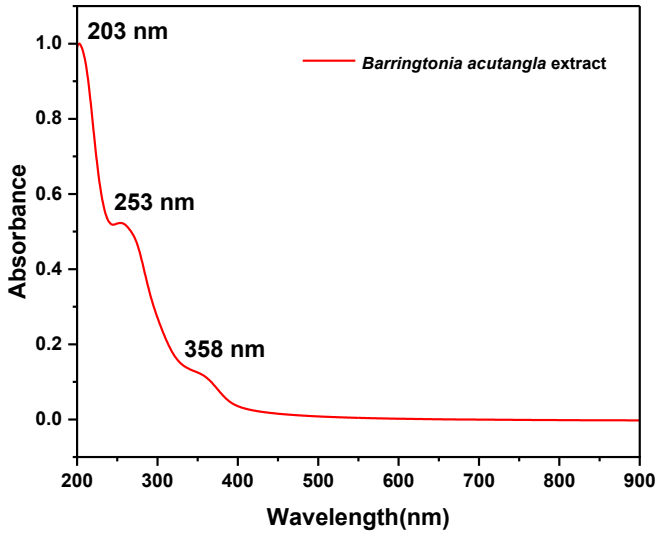

Fig.3 (a) ***UV-Vis spectrum of extract of Barringtonia acutangla***

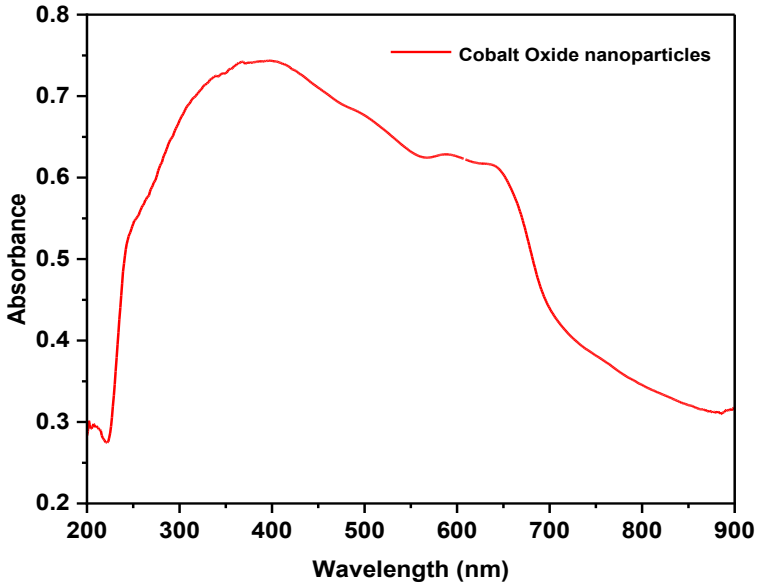

Fig.3 (b) ***Ultraviolet-Visible spectrum of Barringtonia acutangla functionalised Cobalt oxide nanoparticles***

3.2. FTIR studies of Cobalt oxide nanoparticles

Figure 4(a) illustrates the FTIR spectrum of the dried fruit extract of *Barringtonia acutangula*. A prominent broad absorption band around 3500 cm^{-1} is aligned with -OH and –NH stretching modes, likely emanating from amino acids in the extract. Additional peaks at 2933 cm^{-1}, 2851 cm^{-1}, and 2083 cm^{-1} suggest C–H and CH_2 symmetric stretching vibrations. A broad peak at 1651 cm^{-1} could be attributed to N–O asymmetric stretching and C=O stretching indicative of ester groups. A distinct, sharp apex at 1403 cm^{-1} is attributed to aromatic C–C vibrations, commonly found in alkaloid compounds. Peaks around

1000 cm^{-1} can be linked to C–O stretching, while the absorption near 665 cm^{-1} likely corresponds to C–N stretching. The complex signals in the fingerprint region (1500–500 cm^{-1}) reflect multiple vibrational modes, including –CH bending and C–O/C–C stretching, which can be assigned to polyphenols and triterpenoids in the plant extract.

A broad band around 3250 cm^{-1} in Fig 4 (b) is noted as the characteristic peak of O–H stretching modes from hydroxyl groups, which are associated with acidic phytocompounds in the extract. A small band at 2948 cm^{-1} might be due to the C–H and CH_2 vibrational modes, similar to those in the extract. The absorption band near 1651 cm^{-1}, also seen in the extract, again indicates the presence of ester groups. Weak peaks between 1500 and 1000 cm^{-1} suggest symmetric and asymmetric C=O stretching and C–O vibrations, hinting at physical adsorption of CO_2 onto the nanoparticle surface. The signal near 663 cm^{-1} can be attributed to C–N stretching, consistent with retained plant-based functional groups.

Importantly, strong peaks at 570.93 cm^{-1} and 473.55 cm^{-1} are characteristic of O–Co–O and Co–O bond vibrations, confirming the presence of cobalt oxide.[11] Overall, the FTIR data supports the conclusion that phytocomponents in the *Barringtonia acutangula* dried fruit extract caps and stabilises Cobalt oxide nanoparticles during formation, depicting its vital role in the synthesis process.

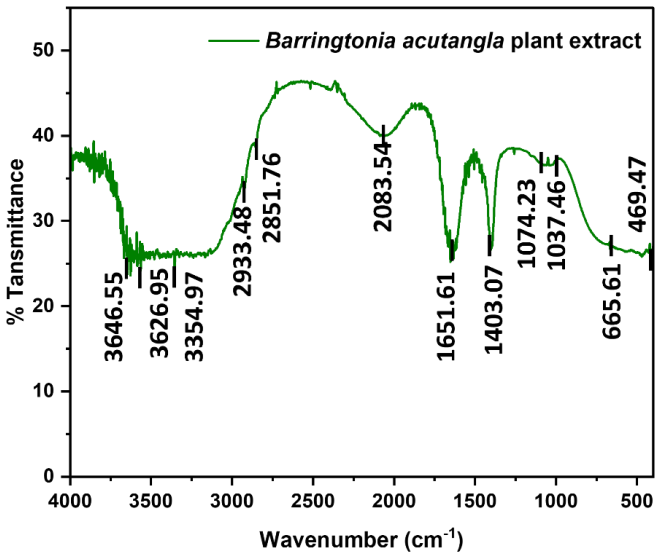

Fig.4 (a) ***FTIR spectrum of Barringtonia acutangla extract***

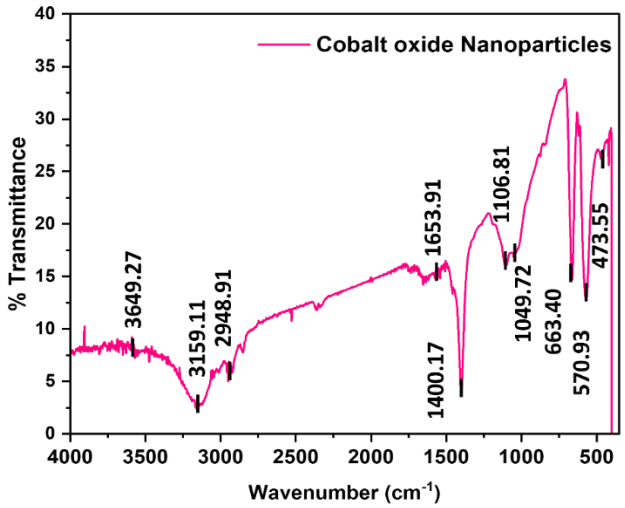

Fig.4 (b) ***FTIR spectrum of Barringtonia acutangla functionalised Cobalt oxide nanoparticles***

3.3.XRD analysis of Cobalt oxide nanoparticles

In Fig.5, five peaks present at 2θ having values 36.5^0, 42.12^0, 61.35^0, 73.34^0 and 77.20^0 correspond to the planes 111, 200, 220, 311 and 222 is in accordance with standard JCPDS Card No. 78-0431 which is attributed to be lattice planes of CoO phase of cobalt oxide nanoparticles with face centered cubic system (FCC) lattice structure [12]. The other peaks at 44.18^0, 59.08^0 and 65.07^0 2θ values correspond to 400, 511, 440 planes of Co_3O_4 lattice phase of Cobalt oxide nanoparticles (JCPDS 42-1467) [13]. XRD indicates coexistence of two phases in the synthesized nanoparticles. The weaker and broad XRD peaks correspond to low crystallinity of the synthesized Cobalt oxide nanoparticles. [14,15]

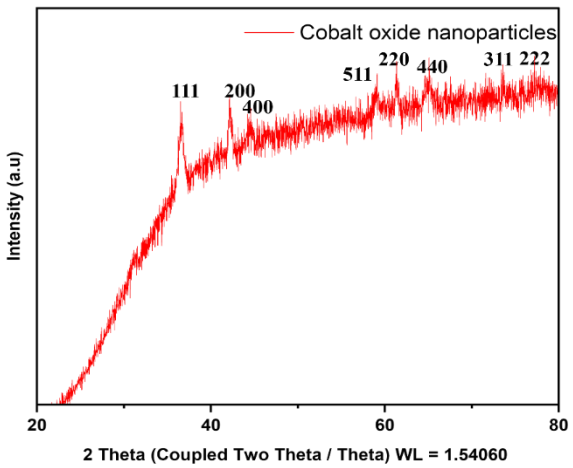

Fig.5 ***XRD behaviour of Barringtonia acutangla functionalised Cobalt oxide nanoparticles***

3.4. SEM and EDAX Analysis

The SEM micrographs in figure 6 (a-d) reveal that the nanoparticles exhibit a rough surface texture characterized by particle agglomeration. This tendency toward aggregation is likely attributable to the nanoparticles' high specific surface area and elevated surface energy inherent to cobalt oxide nanostructures. The EDAX spectrum depicts 53.44 atomic percent oxygen and 46.56 atomic percent cobalt, thereby validating the successful synthesis of pure cobalt oxide nanoparticles. The elemental distribution is depicted in Figure 7 and quantitatively summarized in Table 1.

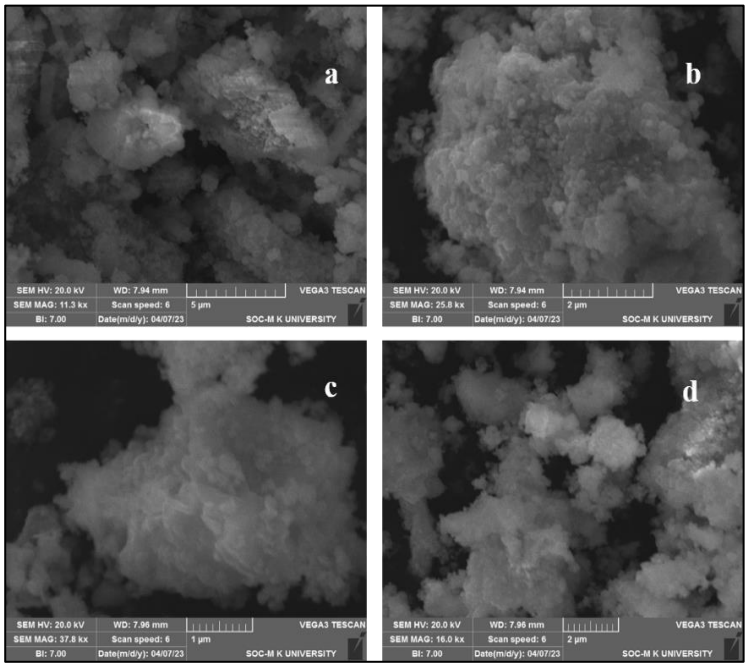

Fig.6 (a-d) ***SEM micrographs of nanocobalt oxide particles at different magnifications***

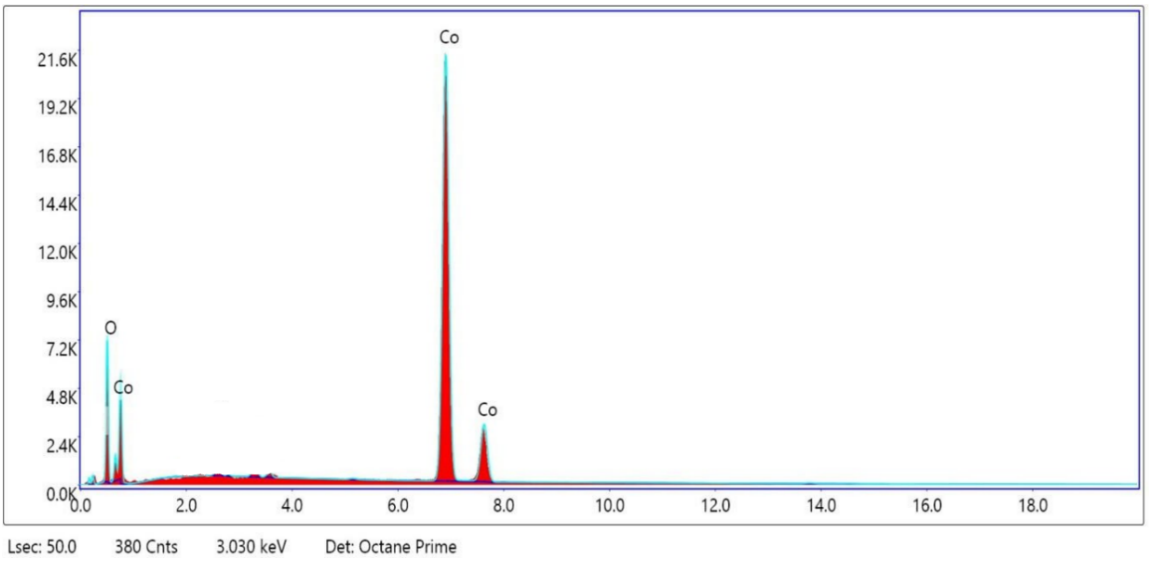

Fig.7 ***Elemental composition of Cobalt oxide nanoparticles***

Table.1. Elemental composition of Barrintonia acutangla functionalised Cobalt oxide nanoparticles

Element	Weight %	Atomic %	Net Int.	Error %	Kratio	Z	A	F
O K	25.19	53.44	739.12	7.81	0.0905	1.1767	0.3438	1.0000
CoK	74.81	46.56	6267.02	1.06	0.6835	0.9332	1.0039	1.0029

3.5. TEM studies

The Transmission Electron Microscopy (TEM) analysis depicted that the synthesized nanocobalt oxide particles possess average size of 43 nm as depicted by statistical size distribution curve in Fig 8(e). While, figure 8 (a-d), shows that the nanoparticles exhibit a combination of spherical and cubic morphologies. This variation in shape suggests the influence of phytochemicals from the *Barringtonia acutangula* extract during the synthesis process, which may act as directing and stabilizing agents.

3.6. Antibacterial activity

Nanoparticles of cobalt oxide have been documented to have a significant function in antibacterial effects. The antibacterial evaluation in aqueous solvent was conducted against pathogenic *Pseudomonas aeruginosa, Escherichia coli* and *Staphylococcus aureus, Bacillus cereus* that are gram negative and grampositive bacteria respectively as illustrated in Figure 9 (a-d). The antibacterial effectiveness, measured by the inhibition zone, showed considerable variation depending on the tested bacterial strains.

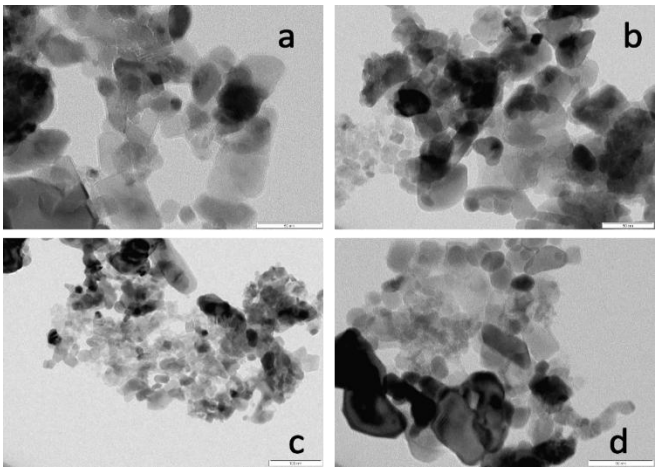

Fig.8(a-d) ***TEM nano images of Cobalt oxide nanoparticles***

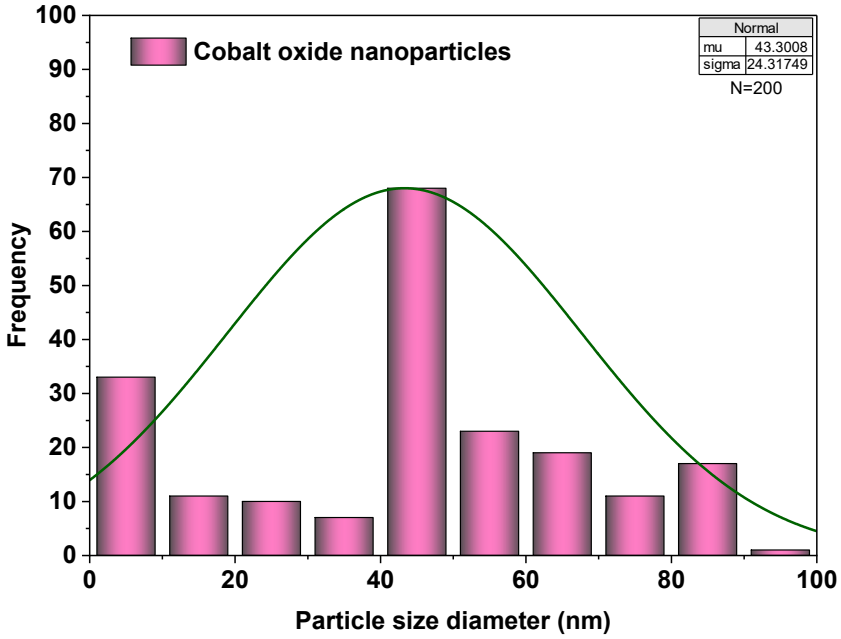

Fig.8 (e) ***Statistical size distribution curve of Cobalt oxide nanoparticles***

3.6.1. Mechanism of Antibacterial action

The ability of nanocobalt oxide particles to act against bacteria is attributed to multiple mechanisms. These include disruption of bacterial membranes, ROS generation (e.g., H_2O_2, O_2^-, •OH), and Co^{2+} ion release, which interferes with protein function and metabolism. Cobalt oxide NPs may also penetrate cells and damage DNA, inhibiting replication. Phytochemicals from *Barringtonia acutangula* extract used in synthesis enhance antimicrobial effects and act as stabilizing agents. The nanoparticles exhibit strong antibacterial activity with minimal toxicity to mammalian cells. Antibacterial test results are shown in Fig. 9 (a–d), with inhibition zones compared in Fig. 10 and detailed in Table 2.

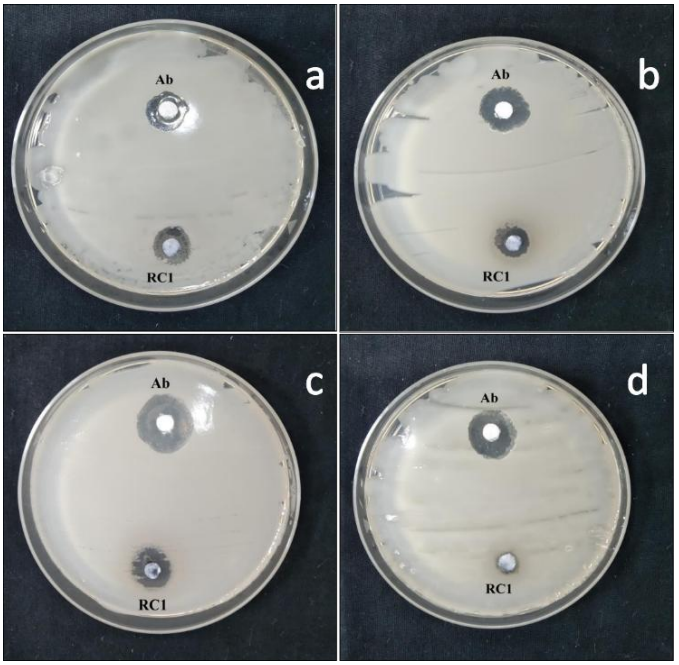

Fig.9 (a-d) ***Antibacterial activity of Cobalt oxide nanoparticles synthesized from Barringtonia acutangla against (a) E.coli (b) S.aureus (c) B.subtilis (d) P.aeruginosa***

Table.2. ***Antibacterial efficacy of Cobalt oxide nanoparticles synthesized from Barringtonia acutangla***

Bacteria	**Inhibition zone in mm**	
	Ab-Ciprofloxacin	**Cobalt oxide Nanoparticles (RC1)**
E.coli	14	12
Staphylococcus aureus	16	11
Bacillus subtilis	18	12
Pseudomonas aeruginosa	16	-

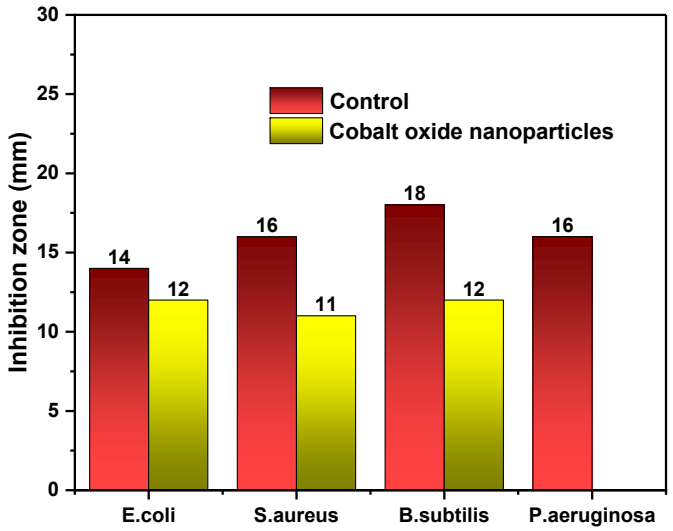

Fig.10. ***Comparison of Zones of inhibition of Cobalt oxide nanoparticles against various test Bacterial strains***

3.7. Total Antioxidant activity

Investigating antioxidant activity is crucial for determining how various substances—particularly natural extracts, dietary components, or synthetic agents—counteract free radicals and minimize oxidative stress, a major contributor to aging, inflammation, and conditions such as cancer, heart disease, and neurodegenerative disorders. The total antioxidant capacity is evaluated using sphectrophotometer using the phosphomolybdenum assay which entails the conversion of molybdenum in its hexavalent state [Mo (VI)] to the pentavalent form [Mo(V)] in low pH, resulting in the generation phosphate/Mo(V) green coloured complex. This complex produces peak at 695 nm. The cobalt oxide nanoparticles demonstrated a total antioxidant activity equivalent to 91.27% ascorbic acid. When the nanocobalt oxide particles have more antioxidant nature higher is the reduction of Mo (VI) to Mo(V) green complex leading to higher absorbance. Higher absorbance reveals higher total antioxidant capacity (TAC). The compilation of the results of antioxidant assay is presented in Table 3 and Figure 11 illustrates correlation between nanoparticle concentration and their percentage antioxidant activity.

$$\% \text{ Antioxidant activity} = \frac{\text{Sample Absorbance}}{\text{Standard Absorbance}} \times 100$$

Table. 3. Anti-oxidant activity of Cobalt oxide nanoparticles

Sample	**Concentration µg/ml**	**OD @ 695 nm**	**% Antioxidant activity**
Ascorbic acid	1000	1.500	-

Cobalt oxide NPs	200	0.381	25.40
	400	0.821	54.73
	600	0.974	64.93
	800	1.222	81.46
	1000	1.369	91.27

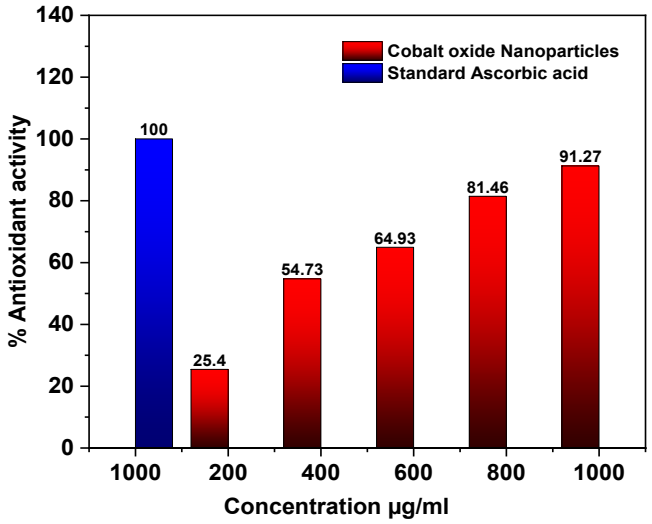

Fig .11. ***Anti-oxidant activity of Cobalt oxide nanoparticles***

3.8. Protein denaturation inhibition activity

Proteins are the essential biomolecule responsible for the normal physiological function of living organisms. Certain factors like oxidative stress, heat and certain chemicals cause denaturation of proteins eventually leads to several diseases like Alzheimer's and ultimately death of living organisms. Hence, drugs which prevents protein denaturation need to be developed. In this aspect, Cobalt oxide nanoparticles was tested for protein denaturation inhibition activity against heat denaturation of proteins. It exhibited Maximum of 59.64 % protein denaturation inhibition activity at 1000 µg/ml concentration. The possible mechanism of protein denaturation inhibition activity may be due to the binding capability of nano cobalt oxide with protein three-dimensional framework which enforces its stabilisation against heat denaturation. The protein denaturation study of Cobalt oxide nanoparticles was given in table 4 and a bar diagram for the protein denaturation study is given in Fig.12.

$$\% \text{ Inhibition } = \frac{Ac - At}{Ac} \text{x } 100$$

Table 4: Protein denaturation inhibition of Cobalt oxide nanoparticles

Sample	**Concentration µg/ml**	**OD @ 660 nm**	**% Inhibition**
Control	-	0.280	-
Cobalt oxide NPs	200	0.249	11.07
	400	0.185	33.93
	600	0.157	43.93
	800	0.144	48.57
	1000	0.113	59.64

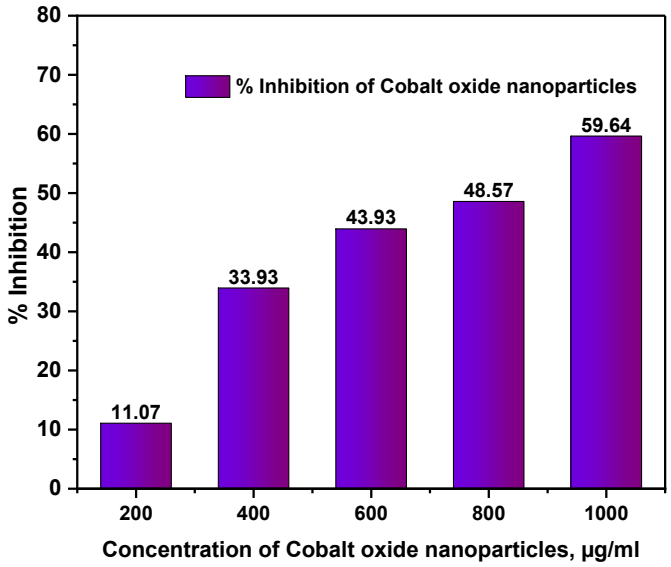

Fig.12. ***Protein denaturation inhibition of nanocobalt oxide particles***

4. CONCLUSION

The phytochemical synthesis of nanocobalt oxide particles using extracts offers a sustainable, eco conscious and affordable solution over traditional physicochemical approaches. Employing the naturally occurring phytochemicals for reduction and stabilization, nanocobalt oxide particles with distinct morphological and structural characteristics was successfully facilitated in this study. Various characterisations were employed to confirm the successful synthesis, crystallinity, size and elemental composition of the nanoparticles. The bioactive compounds from the plant extract not only aided the stabilization of the nanoparticles but also contributed to their biological activity. Importantly, the synthesized Cobalt oxide nanoparticles exhibited promising effects on four different bacterial strains, highlighting their capability to act as effective antimicrobial substances. It also showed excellent antioxidant and appreciable protein denaturation activity. Given their promising properties, green-synthesized cobalt oxide nanoparticles can be further explored for applications in biomedical fields, environmental remediation, and nanotechnology-based industries.

REFERENCES

[1] Patil, S. S., Shedbalkar, U. U., Truskewycz, A., Chopade, B. A., & Ball, A. S. (2018). Nanoparticles for environmental clean-up: A review of potential risks and emerging solutions. *Environmental Technology & Innovation*, 11, 251–269.

[2] Iravani, S. (2011). Green synthesis of metal nanoparticles using plants. *Green Chemistry*, 13(10), 2638–2650.

[3] Ahmed, S., Saifullah, Ahmad, M., Swami, B. L., & Ikram, S. (2016). Green synthesis of silver nanoparticles using *Azadirachta indica* aqueous leaf extract. *Journal of Radiation Research and Applied Sciences*, 9(1), 1–7.

[4] Singh, J., Dutta, T., Kim, K. H., Rawat, M., Samddar, P., & Kumar, P. (2018). 'Green' synthesis of metals and their oxide nanoparticles: applications for environmental remediation. *Journal of Nanobiotechnology*, 16(1), 84.

[5] Rajendran, L., & Muthuraman, G. (2020). Green synthesis and characterization of cobalt oxide nanoparticles using *Solanum nigrum* leaf extract for electrochemical applications. *Materials Research Express*, 7(1), 015054.

[6] Ganesan Vanangamudi, Muthuvel Subramanian, Ganesamoorthy Thirunarayanan, Synthesis, spectral linearity, antimicrobial, antioxidant and insect antifeedant activities of some 2,5-dimethyl-3-thienyl chalcones,Arabian Journal of Chemistry, Volume 10, Supplement 1, 2017, Pages S1254-S1266, ISSN 1878-5352, https://doi.org/10.1016/j.arabjc.2013.03.006.

[7] Md. Nur Alam, Nusrat Jahan Bristi, Md. Rafiquzzaman, Review on in vivo and in vitro methods evaluation of antioxidant activity, Saudi Pharmaceutical Journal, Volume 21, Issue 2, 2013, Pages 143-152, ISSN 1319-0164, https://doi.org/10.1016/j.jsps.2012.05.002.

[8] D.Barreca, C.Massignan, S.Daolio, M.Fabrizio, C.Piccirillo, L.Armelao, E.Tondello, Composition and

microstructure of cobalt oxide thin films obtained from a novel cobalt (II) precursor by chemical vapor deposition, Chem.Mater.13(2001)588–593.

[9] M. Lenglet, C.K.Jørgensen, Reinvestigation of the optical properties of Co_3O_4, Chem.Phys.Lett. 229(1994)616–620.

[10] A. Gulino, P.Dapporto, P.Rossi, I.Fragalà, A novel self-generating liquid MOCVD precursor for Co_3O_4 thin films , Chem.Mater.15(2003)3748–3752.

[11] Naveen, Nirmalesh. (2014). Investigation on physiochemical properties of Mn substituted spinel cobalt oxide for supercapacitor applications. Electrochimica Acta. 125. 404-414. 10.1016/j.electacta.2014.01.161.

[12] Deori, Dr. Kalyanjyoti & Deka, Sasanka. (2013). Morphology oriented surfactant dependent CoO and reaction time dependent Co_3O_4 nanocrystals from single synthesis method and their optical and magnetic properties. CrystEngComm. 15. 10.1039/C3CE41502C.

[13] Ahmad, Md. Hasive & Islam, Md Roxy & Muhammad, · & Islam, Rakibul. (2024). Improved Electrochemical Performance of Co_3O_4 Incorporated MnO_2 Nanowires for Energy Storage Applications. Arabian Journal for Science and Engineering. 50. 10.1007/s13369-024-09421-8.

[14] Muhammad, Hafeez & Shaheen, Ruzma & Akram, Bilal & Abdin, Zain & Haq, Sirajul & Mahsud, Salahudin & Ali, Shaukat & Taj, Rizwan. (2020). Green Synthesis of cobalt oxide nanoparticles for potential biological applications. Materials Research Express. 7. 10.1088/2053-1591/ab70dd.

[15] Manh, D.H. & Nhã, Trần & Le, Phong & Nam, Pham & Thanh, T. & Pham Thanh, Phong. (2023). Determination of the crystalline size of hexagonal $La_{1-x}Sr_xMnO_3$ (x = 0.3) nanoparticles from X-ray diffraction – a comparative study. RSC Advances. 13. 25007-25017. 10.1039/d3ra04018f.